Road Damaging Effects of Dynamic Axle Loads

D. Cebon[1]

ABSTRACT

A number of criteria and associated statistical analysis procedures are proposed for relating the dynamic wheel forces generated by heavy vehicles to road surface damage. The criteria are evaluated in the time domain and therefore require time histories of the dynamic forces generated by all axles of a vehicle. Also required for some of the criteria is the calculation of transient stresses and strains in road structure during the passage of a vehicle. A method for performing this calculation is described. The criteria may be used for evaluating the road damaging effects of simulated or measured wheel forces. In this paper, wheel forces generated by the linked tandem axles of a semi-trailer are simulated and an examination is made of the effects of vehicle speed and road roughness on road damage.

The results indicate that for vehicles operating on stationary random road surfaces typical of highways, road surface damage generally increases steadily with speed. Furthermore, there exist certain speeds at which pitch coupling between axles results in a significant increase in the damage incurred at particular points along the road. For the vehicle examined in this study, the coupling is provided by lightly damped pitching of the load levelling arrangement and the "critical" speeds are found to be approximately 9 m/s and 27 m/s. On smooth roads at high speeds, the increase in dynamic wheel loads with speed is outweighed by the decrease in road surface response. The net effect is a reduction in fatigue damage for speeds greater than 30 m/s.

It is concluded that the dynamic component of wheel forces may reduce significantly the service lives of road surfaces which are prone to fatigue failure. In particular the damage done to approximately five percent of the road surface area during the passage of a vehicle at typical highway speeds may be increased by as much as a factor of four.

1. INTRODUCTION

In recent years, considerable research effort has been concentrated on the measurement and prediction of dynamic wheel loads. An equivalent effort has been concentrated on static analysis of road structures and their failure mechanisms. Very few investigators have examined the relationships between dynamic wheel loads of heavy vehicles and road surface deterioration. The primary aim of dynamic road loading legislation is minimisation of road surface damage so it is essential that these relationships be understood. Only then can road-damage-related vehicle suspension design controls be introduced.

The aims of this article are to establish some road damage criteria and statistical analysis methods suitable for investigating these relationships and to perform a preliminary examination of the road damaging effects of the tyre forces generated by a simple representative semi-trailer vehicle model.

2. CRITERIA FOR EVALUATION OF ROAD DAMAGE DUE TO DYNAMIC AXLE LOADS

2.1 DYNAMIC FORCE CRITERIA USED BY PREVIOUS WORKERS

There is no apparent consensus of opinion in the literature regarding the most appropriate criteria for evaluating the road damaging effects of dynamic tyre forces. Many characteristics of these forces have been measured or calculated in previous studies (see (1) for a more detailed discussion of this literature):

(i) Transfer functions between road roughness and tyre forces (2-5)

(ii) Spectral densities (5-12)

(iii) RMS values (often normalised by static axle loads) (5-10,12-15)

1 Engineering Department, University of Cambridge, England

(iv) Fourth power weighted RMS values (6,10,14,15)

(v) Transient values (due to discrete surface irregularities) (3,4,11,16-20)

(vi) Probability distributions (5,8,10,11,13,20)

(vii) Percentage of road subjected to forces lying in given intervals (20)

(viii) Dynamic load sharing between linked axles (6,10,14)

(ix) Longitudinal contact forces (2,11)

(x) Ground motion near to road (due to surface waves) (17,19)

(xi) Vertical subgrade pressure below a discrete surface irregularity (21).

Very few workers have considered the relationships between fluctuating wheel loads and road surface damage. One notable exception is Savage (22) who postulated that cracking at the "downstream" end of concrete pavement slabs (near joints) is due to transient tensile stresses caused by the sudden release of load as an axle passes onto the next slab.

The most important recent contribution was made by Sweatman (10,14) who used a hub-mounted wheel force transducer to measure the dynamic loads generated by one wheel on each of 9 different (Australian) commercial vehicles. Tests were performed for a range of speeds, tyre pressures and road surfaces. Assuming that the wheel forces followed a Gaussian distribution and using the "fourth power law"[1] for road damage, he calculated the "road stress factor":

$$\Phi = KP_s^4\,[1 + 6\bar{s}^{\,2} + 3\bar{s}^{\,4}]$$

$\bar{s}$ = Dynamic load coefficient = σ/P_s

σ = Standard deviation of wheel load

P_s = Mean axle load

K = Constant

Sweatman defined the dynamic road stress factor by $\upsilon = \Phi/KP_s^4$ and suggested that this factor should account for the damaging effects of the dynamic component of the wheel loads. For typical highway conditions of roughness and speed, this factor was found to vary between 1.11 and 1.46, depending on the suspension system (10).

Recognising the importance of the relatively few, very large wheel forces, Sweatman also calculated the stress factor associated with the 95th percentile forces:

$$\Phi_{95} = (1 + 1.645\bar{s})^4$$

This factor was found to vary between 2.21 and 4.37 for the highway operating conditions of his experiment.

Sweatman also examined the average dynamic load sharing between axles:

LSC = Load Sharing Coefficient = $2n\bar{z}/Mg$

n = number of axles in group

$\bar{z}$ = mean wheel force

Mg = total axle group static load.

Up to 21% deviation from perfect load sharing (LSC=0.79) was displayed by one tandem suspension system but most suspensions deviated by less than 10%.

Ervin et al (6) performed similar tests in the USA and obtained qualitative agreement with Sweatman's results[2].

Two important factors have been overlooked by these studies:

(i) The "fourth power law" used in Sweatman's analysis (10,14) was developed on the basis of the static axle weights of the vehicles in the AASHO test (23). It refers to global deterioration of the road surface rather than local failure and so it cannot simply be extended

1 The "fourth power law" stems from the AASHO road test (1958-60) (23) from which it was concluded that the decrease in "pavement serviceability" caused by a heavy vehicle axle could be related to the fourth power of its static load. A static load αP_o is assumed to be equivalent to α^4 applications of the standard wheel load P_o.

2 It was not possible for the American test conditions to match exactly those of the Australian study.

to the evaluation of dynamic wheel forces. Also the general validity of the "fourth power law" is questionable; this is discussed in detail in (1).

(ii) Dynamic forces are applied to the road surface by all wheels of a vehicle. A point on the road surface along a wheel path will experience an impulse due to each passing wheel and the total damage done by the vehicle at that point will depend on the accumulated damage due to each wheel load. The peak loads (which inflict most damage) will result from specific road roughness features and therefore will occur repeatedly in the same general locations on the pavement (in the vicinity of the roughness feature) (6). It may be expected that road surface degradation caused by wheel loads would start at these locations. It is necessary therefore to examine the damage incurred at specific points along the road and it is of doubtful benefit to examine wheel force statistics such as peak or RMS values of a single axle, or the average dynamic load sharing between axles.

There is clearly a need for some criteria which relate dynamic forces to damage at particular points along the road surface. These criteria should take into consideration the mechanisms of failure of typical road structures.

2.2 FAILURE MECHANISMS OF ROAD STRUCTURES

Road structures may be classified as flexible, composite or rigid. A flexible pavement consists of one or more layers of flexible (bituminous) material supported by a granular subgrade. Composite pavements consist of a flexible surface layer supported by a stiff (concrete) base and rigid road surfaces consist of a layer of concrete on a granular foundation. Rigid pavements may be further classified according to their arrangement of steel reinforcement and joints.

Each of these road types has a number of characteristic failure mechanisms. According to Rauhut, Roberts and Kennedy (24,25), the most important of these are[1]:

(i) Fatigue cracking for all types of pavements

(ii) Permanent deformation (longitudinal rutting) for flexible and composite pavements

(iii) Reduced skid resistance for flexible and composite pavements

(iv) Low temperature cracking for flexible pavements

(v) Reflection cracking for composite pavements

(vi) Faulting, spalling, low temperature and shrinkage cracking, blow ups, punchouts and steel rupture for rigid pavements, depending on their structural category.

Each failure mechanism is affected by many factors including the roadway design and construction methods, the material properties of each constituent layer (these are generally discontinuous, nonlinear and anisotropic), the traffic loading and the environmental conditions throughout the service life (25).

2.3 FAILURE CRITERIA FOR FLEXIBLE PAVEMENT ANALYSIS

Current practice in many countries is to design flexible road structures for resistance to failure by fatigue and rutting (26). Elastic or viscoelastic layer theory or finite element methods are used to calculate stresses and strains in the road due to a static, standard wheel load (usually 40kN). The "fourth power law" is used frequently to estimate the expected number of standard wheel loads (in mixed traffic) during the service life. Experimental fatigue and permanent deformation characteristics of the road materials (27) are used in conjunction with one or more of the following design criteria to determine pavement layer thicknesses.

(i) **Rutting:** Subgrade compressive stress or strain, vertical surface deflection

(ii) **Fatigue:** Horizontal tensile stress or strain[2], volumetric strain, shear strain and shear stress.

Although considerable research effort has been concentrated on prediction of pavement failure, agreement between theory and experiment is often unsatisfactory. There are numerous complicating factors including "healing" of bituminous materials in rest periods between load pulses (28,29), the distribution of wheel paths across the road (26,28), extreme sensitivity of material properties to climatic conditions particularly

1 The terminology used here is defined in (25).

temperature (26-28,30-32), inaccuracy of the "fourth power law", inadequacies of pavement structural models and the variable nature of the applied loads. Thrower (28) summarised the difficulties:

> *"The conventional methods adopted to assess the risk of fatigue failure in flexible pavements are unsatisfactory in many respects; they are conceptually vague, the laboratory experimental data are inadequate to define an appropriate criterion uniquely, and the mechanism of pavement fatigue failure postulated is not adequately supported by road experience in Britain. In their basic form, the models generally yield gross underestimates of the fatigue life of typical pavements ...."*

It is in this context of uncertain roadway design practice that criteria for evaluating dynamic wheel loads must be established.

2.4 FOUR ROAD-DAMAGE-RELATED CRITERIA FOR ASSESSING DYNAMIC WHEEL LOADS

In order to quantify the effects of fluctuating wheel loads on pavement deterioration it is necessary to examine the accumulated damage due to all axles of a passing vehicle at specific points on the road surface. Loss of serviceability will be governed by a small proportion of locations at which large damage occurs.

The procedure adopted in this study was to divide the road surface along each wheel path into a number of equal segments. The segments were sufficiently short to enable the resolution of peak forces at the highest frequency of interest. The accumulated damage at each station due to the passage of a vehicle was calculated by one of criteria described below.

2.4.1 Aggregate Force Criterion

Let the force applied by wheel j to station k on the road surface be P_{jk}. The Aggregate Force at station k $\{F_k\}$ is defined by

$$F_k = \sum_{j=1}^{N_a} P_{jk} \quad k = 1, 2, 3 \ldots N_s \tag{1}$$

N_a = Number of axles

N_s = Total number of stations along wheel path.

We expect $\{F_k\}$ to be a Gaussian random variable, since the individual axle loads are Gaussian in practice (10,12). $\{F_k\}$ should have a mean value equal to the gross vehicle weight and a variance dependent on the dynamics and speed of the vehicle, the coupling and spacing of its axles and the road roughness.

2.4.2 Fatigue Weighted Stress Criterion

As a first approximation, we assume that the maximum damaging stress in the flexible surface layer of a road structure is proportional to the average compressive stress in the tyre contact area. Stress-related fatigue characteristics have been measured, under conditions of fluctuating force, for bituminous materials (33) and cement treated materials (34). Exponential relations of the form

$$N = k_1 \sigma_t^{-n_1} \tag{2}$$

have been reported (k_1 and n_1 are mixed constants, σ_t = stress amplitude, N = cycles to failure). n_1 takes values between 2.5 and 8.1 for asphalts (33).

Using Miner's hypothesis for the accumulation of fatigue damage (27-29), we may estimate a quantity related to the proportion of the total fatigue life used at station k due to the passage of the vehicle:

$$L_\sigma k = 100 \sum_{j=1}^{N_a} (1/N_{jk}) \ (\%) \quad k = 1, 2, 3 \ldots N_s \tag{3}$$

where, from (2),

$$N_{jk} = k_1 \left(P_{jk}/A_j\right)^{-n_1}$$

A_j = *nominal contact area of tyre j.*

A point on the road is considered to have reached the end of its useful life when $L_{\sigma k}$ reaches 100%.

Typical values of k_1 and n_1 were obtained from (33) for bituminous concrete with 5.7% (by mass) asphalt binder.

---

2 Elastic layer and finite element calculations generally indicate that maximum tensile strains occur at the bottom of the flexible surface layer on the axis of the load, implying upwards propagation of cracks. Thrower (28) noted that this failure mechanism is not well supported by observations of core samples taken from roads in Britain, where cracks almost invariably originate at the top surface and extend downwards.

$k_1 = 2.8 \times 10^{19}, \; n_1 = 4.8$

$\{L_{ok}\}$ will be a random variable, however the exponential form of the fatigue relation (2) will result in a skewed probability distribution which will no longer be Gaussian.

The criteria discussed in the two preceding paragraphs grossly oversimplify the relationship between the applied loads and damage to the road structure. Using the method described in Section 3 it is possible to calculate the transient stresses, strains and deflections at a point in the road structure as a vehicle passes by. This method may be used to evaluate the stresses and strains needed for the more realistic road damage criteria described in the next two paragraphs.

2.4.3 Tensile Strain Fatigue Criterion

The most popular criterion (cited in the road damage literature) for estimating the fatigue life of flexible pavements is the tensile strain at the bottom of the asphalt surface layer. Relations between the amplitude of applied tensile strain (ε_t) and number of cycles to failure (N) of asphalt laboratory specimens have been shown to take the form (26-29,33,35)

$$N = k_2 \, \varepsilon_t^{-n_2} \qquad (4)$$

k_2 and n_2 are mix constants. n_2 may vary between 1.9 and 5.5 (27,33,35) The mix parameters used in this study correspond to a typical UK rolled asphalt wearing course with 7.9% binder (by mass) (27).

$k_2 = 1.3 \times 10^{-14}, \; n_2 = 5.1$

Following the same approach as in Section 2.4.2, we may estimate the proportion of the total fatigue life used at station k (L_{ek}) as a result of the strain history caused by the passing vehicle. In this case, however, the "bow wave" and "wake" which accompany a moving load on the road surface (6,15,30,32,36) result in three positive tensile strain peaks (i=1,2,3) associated with each wheel.

$$L_e k = 100 \sum_{j=1}^{N_a} \sum_{i=1}^{3} (1/N_{ijk}) \;(\%) \quad k = 1, 2, 3 \ldots N_s \qquad (5)$$

where N_{ijk} is given by (4) and ε_t is calculated from a theoretical roadway model.

2.4.4 Permanent Deformation Criterion

Assuming that permanent deformation of the road surface is related to the magnitude of the applied loads we might anticipate some variation in rut depth along a road due to fluctuating wheel forces. In the calculations used in this study the subgrade compressive stress history σ_{ck} at stations along the road was used to estimate the local increase in permanent deformation due to the passage of a vehicle.

Majidzadeh et al (37) showed that the permanent strain (ε_p) of asphalt specimens after N cycles may be estimated (for a wide range of asphalt mixes) from the applied stress (σ_c) and the effective modulus (E*) according to

$$\varepsilon_p = k_3 \, (\sigma_c / E*)^{n_3} N^m \qquad (6)$$

$k_3 = 3.6$

$n_3 = 1.08$

$m = 0.13 - 0.27$

E* depends on the rate of loading.

Peattie (26) and Van de Loo (38) used $n_3 = 1$ thereby assuming that permanent strain is proportional to the average strain in the asphalt layer. The permanent deformation at station k on a layer of thickness d due to a single stress pulse of magnitude σ_{cjk} may be estimated from

$$\delta_{pjk} = k_3 \, d \, (\sigma_{cjk} / E*)^{n_3} \qquad (7)$$

The total increase in permanent deformation[1] at station k may be calculated according to

$$\Delta_{pk} = \sum_{j=1}^{N_a} \delta_{pjk} \quad k = 1, 2, 3 \ldots N_s \qquad (8)$$

where σ_c is calculated for the roadway model.

2.5 STATISTICAL ANALYSIS

In the previous section, it was noted that peak wheel forces and hence most roadway deteriora-

1 It should be noted that this calculation does not account for permanent deformation in the subgrade, which is expected to contribute up to 46% of the total deformation of UK roads and up to 68% for US conditions (26). A more elaborate roadway model than the one used in this study is needed to enable the calculation of permanent strains in each pavement layer.

tion may be expected to occur in the vicinity of specific road roughness features. We may postulate that the road surface would become unserviceable when a small proportion of its total surface area (say 1% to 5%) became seriously damaged. The damage incurred at this small proportion of points during the passage of a particular vehicle may be determined from the cumulative probability density function of the road damage measure of interest. For example, 5% of the surface area of the road (along the wheel tracks) is subjected to aggregate force levels greater than the 95th percentile aggregate force.

3. MODELLING ROADWAY RESPONSE

Evaluation of the two criteria discussed in Sections 2.4.3 and 2.4.4 requires a mathematical model of the dynamic response of the road structure to a set of randomly fluctuating forces, moving along its surface.

Many models have been used for the analysis of the dynamic response of roads (39). They fall into two main categories:

(i) A beam or plate supported by massless springs (Winkler foundation) (40-44) or supported by a halfspace (40,41). The Winkler foundation may be modified to include the effects of inertia (45,46).

(ii) A structure comprising one or more layers of elastic or viscoelastic material (39,41,47-50).

The models vary in complexity according to the nature of the layers (elastic, damped elastic, viscoelastic) and the surface loading (moving, constant, harmonic..). However, very few layered models include the effect of moving loads and none, the effects of moving loads and viscoelasticity (39). The literature in this field has been reviewed extensively by Hunt (39). This will not be repeated here.

3.1 CALCULATION OF THE TIME DOMAIN RESPONSE OF A SEMI-INFINITE, LINEAR CONTINUOUS SYSTEM TO MOVING RANDOM LOADS

3.1.1 Transfer Function

Consider a stationary load p(x,y,t) on the surface (z = 0) of a semi-infinite linear system. We assume a harmonic input at angular frequency ω

$$p(x,y,t) = P(x,y)\, e^{i\omega t} \tag{9}$$

and consider separable steady state solutions of the equations of motion of the system which take the form

$$\phi(x,y,z,t) = \Phi(\underline{R},\omega)\, e^{i\omega t} \tag{10}$$

where ϕ (x,y,z,t) is the response of interest (stress, strain, displacement, etc.) and $\underline{R} = x\underline{i} + y\underline{j} + z\underline{k}$ is the position vector of a measuring point from the load.

The transfer function $H(\underline{R}, \omega)$ is given by

$$H(\underline{R},\omega) = \Phi(\underline{R},\omega)/P(x,y) \tag{11}$$

This may be determined from the equation of motion of the system by Laplace or Fourier transform techniques (see for example (1,42)).

3.1.2 Impulse Response

The response $h_A(t) = h(\underline{R}_A, t)$ of the system at point A to a unit impulse applied at $\underline{R} = 0$, is given by the Fourier transform relationship

$$h_A(t) = (1/2\pi)\int_{-\infty}^{\infty} H(\underline{R}_A, \omega)\, e^{i\omega t} d\omega \tag{12}$$

In practice this can be calculated approximately by the one dimensional inverse discrete Fourier transform (IDFT)

$$h_A(t = r\Delta t) = (1/N\Delta t)\sum_{k=0}^{N-1} H(\underline{R}_A, \omega_k)\, e^{i2\pi kr/N}$$

$$\text{where} \quad r = 0, 1, 2 \ldots (N-1) \tag{13}$$

$\omega_k = 2\pi k/N\Delta t$

Δt = time increment

$N/2$ = Number of frequency intervals at which $H(\underline{R}_A, \omega)$ is sampled.

The IDFT (13) will produce a faithful representation of the true impulse response providing Δt is sufficiently small so that $H(\underline{R}_A, \omega = \pi/\Delta t) \to 0$. The accuracy can be improved by multiplying $H(\underline{R}_A, \omega)$ by a data window $W(\omega)$, where $W(\omega) \to 0$ when $\omega \to \pi/\Delta t = 1$ when $\omega = 0$.

The result will be the true impulse response function convolved with the Fourier transform of $W(\omega)$. A Gaussian data window is particularly suited to this purpose (51), and was used in the sample calculation in this study.

3.1.3 Total Time Domain Response at a Fixed Point

It is now possible to determine the total response at a particular fixed point in the road as a fluctuating load p(x,y,t) moves by at steady speed.

p(x,y,t) may be divided into a series of impulses in time of duration $d\tau$ and magnitude $p(x,y,\tau)d\tau$. Consider the response at time t at a point A which is at rest at position $\underline{\rho}$ from the stationary origin (Figure 1). An impulse of magnitude $p(x,y,\tau)d\tau$, applied at time t contributes an amount

$$h\,(\underline{r}\,(\tau), t-\tau)\; p\,(x,y,\tau)\; d\tau, \quad where\ \underline{r}\,(\tau) = \underline{\rho} - V\tau\underline{i}$$

to the response at time t. A short time $\delta\tau$ later the load will have moved a distance $V\delta\tau\underline{i}$ $\underline{r}\,(\tau+\delta\tau)$ and the contribution to the response at point A at titme t will be

$$h\,(\underline{r}\,(\tau+\delta\tau), t-\tau-\delta\tau)\; p\,(x,y,\tau+\delta\tau)d\tau$$

The total response $\phi(\underline{\rho},t)$ at time t will be the sum of all such contributions up to time t.

$$\phi(\underline{\rho},t) = \int_{-\infty}^{t} h\,(\underline{r}\,(\tau), t-\tau)\; p\,(x,y,\tau)d\tau \qquad (14)$$

An alternative version of (14) is obtained by putting $\theta = t - \tau$

$$\phi(\underline{\rho},t) \approx \int_{0}^{\theta_0} h\,(\underline{r}\,(t) + V\,\theta\,\underline{i},\theta) p\,(x,y,t-\theta)d\theta \qquad (15)$$

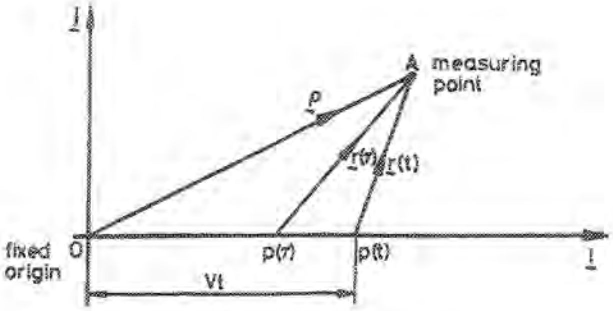

Notation for calculation of the total response of the road model at "measuring" point A. The load p(t) moves along the i axis at steady speed V

FIGURE 1

$$where\ \underline{r}\,(t) = \underline{\rho} - Vt\underline{i} \qquad (16)$$

and $|h|$ *is negligible* for $\theta \geq \theta_0$

In order to perform this calculation by digital computer we let

$$\theta_j = j\Delta\theta \quad and \quad \theta_0 = N_0\Delta\theta \qquad (17)$$

Eq. 15 then becomes

$$\phi(\underline{\rho},t) \approx \Delta\theta \sum_{j=0}^{N_0} h\,(\underline{r}\,(t) + V\theta_j\underline{i}, \theta_j)\; p\,(x,y,t-\theta_j) \qquad (18)$$

For n applied loads moving at the same velocity (eg a n-axled vehicle) the principle of superposition can be used and this result can be extended to

$$\phi(\underline{\rho},t) = \Delta\theta \sum_{i=1}^{n} \sum_{j=1}^{N_0} h\,(\underline{r}_i + V\theta_j\underline{i}, \theta_j)\; p_i\,(x,y,t-\theta_j) \qquad (19)$$

Note that calculation of the impulse responses (13) need be performed once only for each (y,z). The impulse responses may subsequently be used to calculate the response of the system to any moving loads. Any responses of the model (displacements, velocities, strains, stresses, etc.) may be calculated in this way from the appropriate transfer functions.

3.2 SIMPLE BEAM MODEL

A two dimensional Euler beam supported by a damped, elastic (Winkler) foundation was used in this study to model road surface response (Figure 2). Although the model is slightly unrealistic, the methods developed here may be extended to substantially more complex road models in future. The calculation is intended to be a sample only, with the objective of establishing the expected trends in road damage. The equation of motion of the model, the parameter values and the method of solution are described in (1).

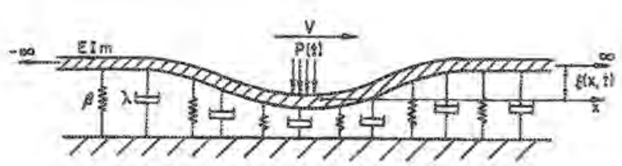

Two dimensional roadway model

FIGURE 2

Figure 3 shows the displacement transfer functions | H(x, ω) | at a number of stations along the beam. The corresponding impulse responses, calculated according to Equ. 13 are shown in Figure 4. For the criteria described in section 2.4.3 and 2.4.4 it is necessary to compute impulse responses for the extreme fibre direct strain in the beam and the subgrade compressive stress.

4. SIMULATION OF DYNAMIC AXLE LOADS

4.1 VEHICLE MODEL

It was desired to simulate, as realistically as possible in the time domain, dynamic wheel forces suitable for analysis using the road damage criteria discussed previously. In view of the importance of assumptions regarding suspension spring characteristics (1,12) it was considered necessary to use nonlinear models.

A six-degrees-of-freedom, two dimensional mathematical model of a linked tandem-axle semi-trailer was developed (see Figure 5). Important features of the model are:

Tyres:

(i) Linear springs in parallel with light viscous dampers

(ii) Simple contact patch averaging for envelopment of short wavelength road roughness

(iii) Departure of wheels from the road surface

Suspensions:

(i) Four-leaf suspension system with nonlinear leaf spring elements connected by a "massless" load leveller

(ii) Frictionless load leveller pivot

(iii) Sprung mass modelled by a rigid 11 tonne mass (1/2 vehicle only).

The equations of motion and numerical data for the vehicle model are provided in (1). The equations of motion were solved in the time domain by numerical integration according to the validated methods described in (1,52).

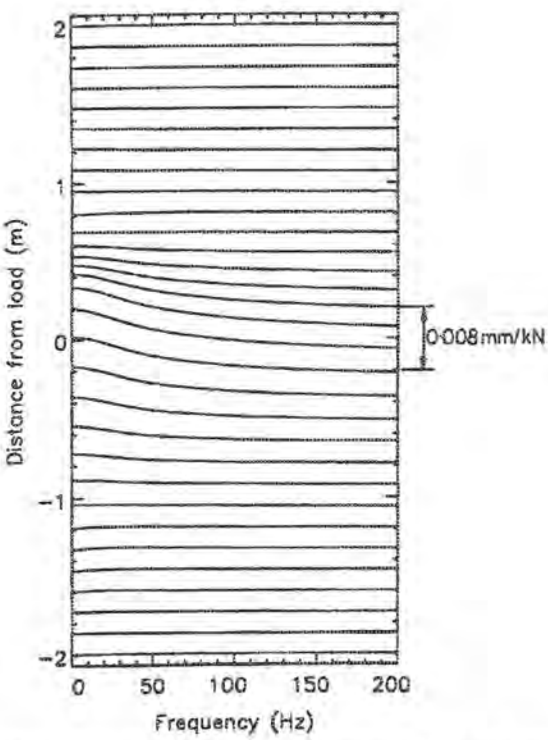

Displacement transfer functions | H(x,ω) | at a number of stations along the beam

FIGURE 3

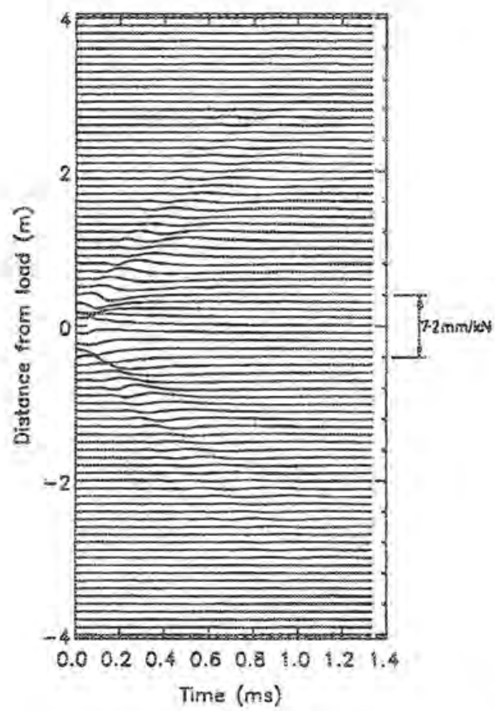

Displacement impulse response functions h(x,t) at a number of stations along the beam

FIGURE 4

4.2 ROAD SURFACE ROUGHNESS

Inputs to the vehicle model were the profiles of two typical random roads and a 12 mm step. The random road profiles had "good" and "very good" roughness spectral densities according to the two-index classification in (53). These will be known hereafter as profiles 1 and 2 respectively.

The one-dimensional inverse FFT method described in (1,54) was used to generate stationary, Gaussian random sequences with the desired spectral densities.

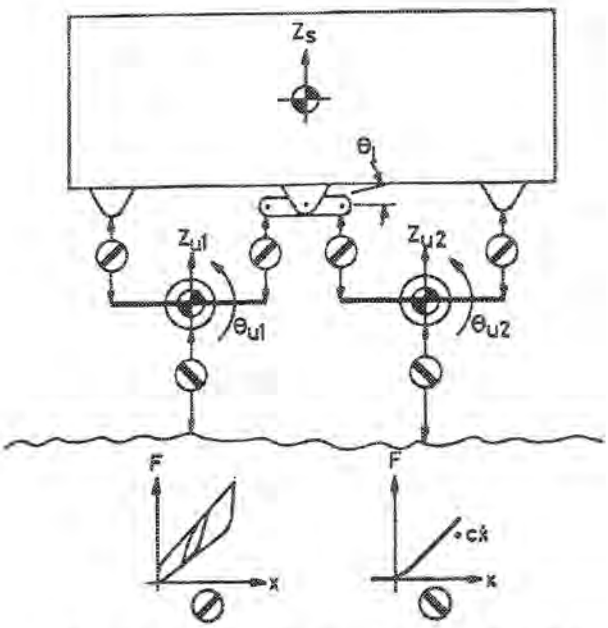

Tandem axle trailer suspension model

FIGURE 5

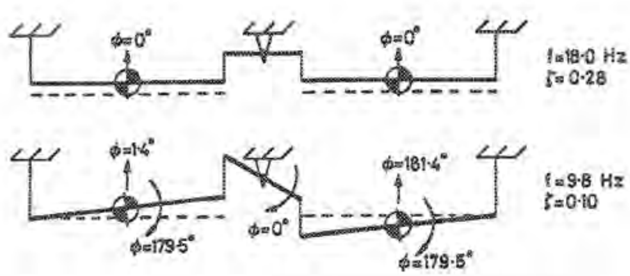

The magnitude of the Eigenvector has been drawn with the sign of the real part of each coordinate response. The phase of each coordinate is indicated by φ

Natural modes of the "four-leaf" trailer suspension model

FIGURE 6

4.3 NATURAL MODES OF THE LINEARISED VEHICLE MODEL

Prior to the nonlinear time domain study, the mathematical vehicle model was linearised by replacing the nonlinear suspension and tyre elements with equivalent linear springs and dashpots (1,52).

The method described in (1) was used to determine the natural frequencies, damping ratios and mode shapes. Table 1 describes the natural modes in the frequency range affecting the tyre forces. Two of the important mode shapes are sketched in Figure 6.

5. SAMPLE RESULTS

Time histories of the tyre forces generated by the trailer suspension model were calculated at a number of speeds (between 5 m/s and 40 m/s) on the three road profiles described in section 4.2. Each of the four criteria was used to evaluate the road damage at equally spaced stations along the wheel path. The station spacing was $\Delta x = V/100$ m for the random profile tests and $\Delta x = V/300$ m for the step inputs (V = vehicle speed m/s).

5.1 AGGREGATE FORCE CRITERION

The aggregate forces $\{F_k\}$ were calculated according to (1). The distribution of these forces for the vehicle traversing road profile No. 1 at a speed of 30 m/s is shown in Figure 7(a). The theoretical Gaussian "bell-shaped" curve with the same mean and standard deviation as the measured data is also shown. The aggregate forces match the normal distribution accurately. This is confirmed by

Table 1 – Natural modes of the linearised vehicle model

Frequency (Hz)(1)	Damping ratio(2)	Description of mode
18.0	0.28	Axles bouncing in phase, sprung mass stationary
9.8	0.10	Axles bouncing in antiphase, load leveller pitch.
2.3	0.03	Sprung mass and axles bouncing in phase.

Note for Eigenvalue $\lambda = -\alpha \pm i\omega$

(1) The natural frequency is defined by $\omega_n = \sqrt{\omega^2 + \alpha^2}$

(2) The damping ratio is defined by $\zeta = \alpha/\sqrt{\omega^2 + \alpha^2}$

the probability paper plot (Figure 7(b)) where the experimental results closely follow the theoretical straight line for Gaussian data.

In accordance with section 2.5 the cumulative probability distribution was used to calculate the 95th, 98th and 99th percentile aggregate force levels as a function of vehicle speed (Figure 8). Small peaks in each curve can be seen at speeds of 9 m/s and 27 m/s. At these speeds, both unsprung masses reach maximum force levels in their 9.8 Hz antiphase bounce cycle (see Table 1) at the same locations on the road surface[1]. In Figure 9, the aggregate forces for all three road profiles (Profiles 1 and 2, and 12 mm step) have been normalised by the gross vehicle weight. For the random profiles the 95th, 98th and 99th percentile aggregate forces are plotted, whereas for the step input tests, the largest peak value is plotted since it is considerably greater than the second largest peak (see Figure 10).

Within the range of highway speeds, some points along the road may be subjected to aggregate forces up to 50% greater than the gross vehicle weight, depending on the roughness of the surface and the speed of the vehicles.

The peak values for the step response tests do not occur at the same speeds as for the random tests. This may be attributed to two factors:

(i) The dynamic response of the vehicle largely depends on the time interval between each tyre encountering the step. At some speeds the vehicle response will "tune in" to the frequency associated with this time interval.

(ii) The aggregate force at a point depends on each axle load that passes by. As a result, the maximum aggregate force will not necessarily occur at the same location as the maximum force generated by either axle, especially in transient input tests.

For this vehicle the combined effects of these factors results in the maximum aggregate force occurring approximately 1.5 m downstream of the step for speeds less than 22.5 m/s and on the edge of the step for $V \geq 22.5$ m/s (Figures 9 and 10). Other factors that complicate the prediction of "critical" speeds in the step response tests are the damping and nonlinearity of the tyres and the nonlinearity of the leaf springs.

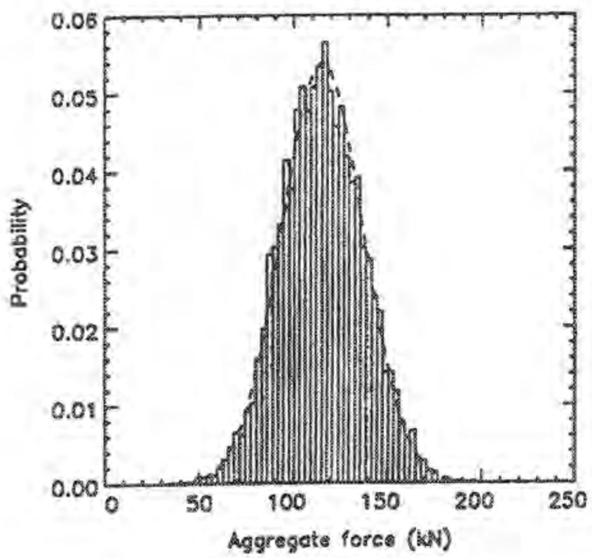

a) Probability distribution - - - - = Gaussian

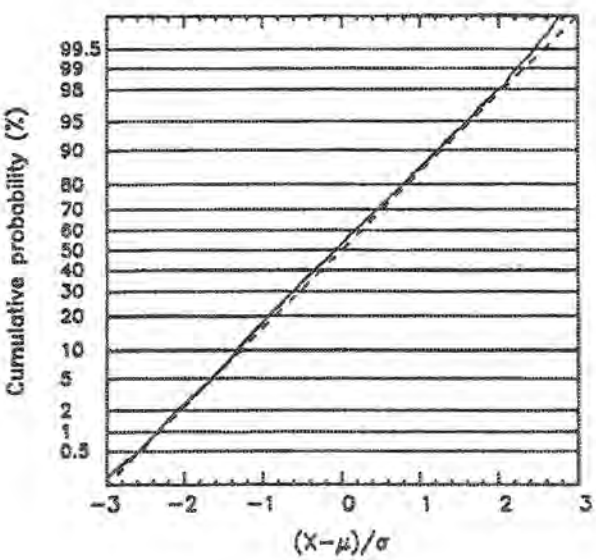

b) Probability paper plot - - - - = Gaussian

Distribution of the aggregate forces generated by the vehicle model travelling at 30 m/s on a road profile No. 1

FIGURE 7

1 At 27 m/s, the antiphase bounce mode undergoes 1/2 of its 9.8 Hz cycle while travelling one wheelbase length (1.4 m). At 9 m/s, 1.4 m is travelled in 1.5 cycles.

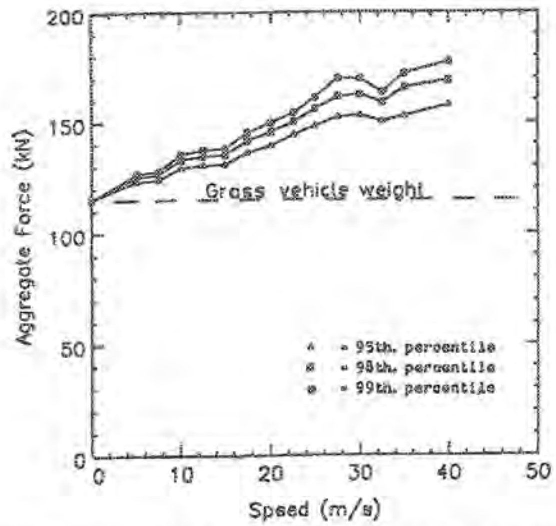

Upper percentile aggregate forces generated by the vehicle model travelling on road profile No. 1

FIGURE 8

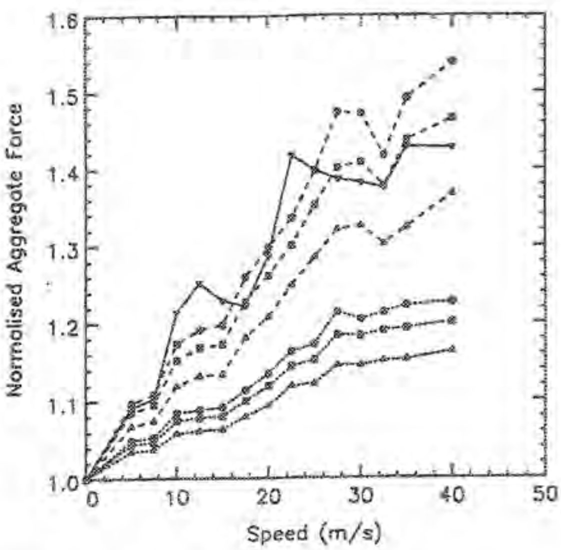

= peak value due to 12mm step,
= random road profile 1,
= random road profile 2,

▲ = 95th. percentile
■ = 98th. percentile
● = 99th. percentile

Aggregate forces generated by the vehicle model travelling on the three road profiles. (all aggregate forces have been normalised by the gross vehicle weight

FIGURE 9

5.2 FATIGUE WEIGHTED STRESS CRITERION

The fatigue weighted stress criterion (section 2.4.2) was used to determine the proportion of the service life used at the same points along the road as discussed in the previous paragraph. The distribution of fatigue life usage for the vehicle travelling on road profile 1 at 30 m/s is shown in Figure 11. The fatigue law (2) skews the distribution so that it is no longer Gaussian.

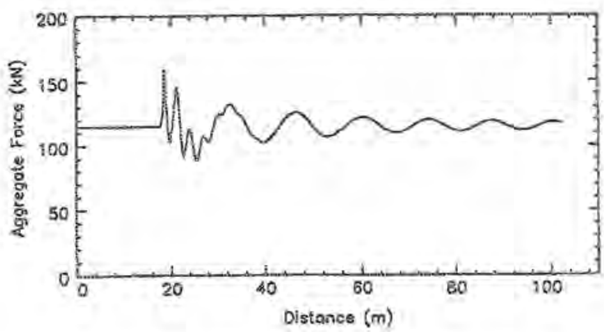

Aggregate forces generated by the vehicle model during passage over a 12 mm step at 30 m/s

FIGURE 10

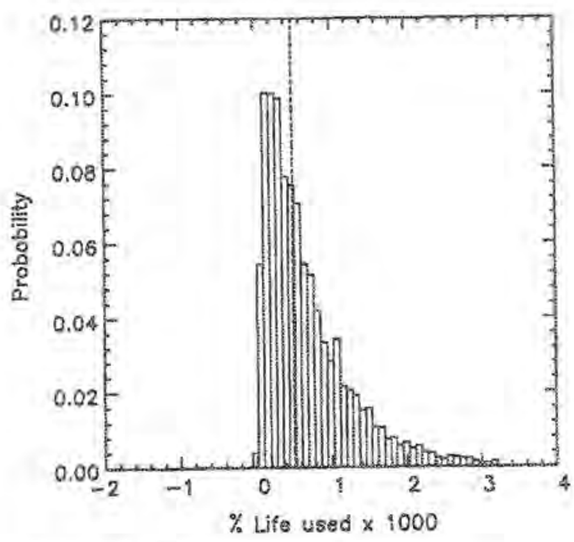

— · — · — · — = Non-dynamic life usage.

Probability distribution of fatigue life usage, determined by the fatigue weighted stress criterion, due to the passage of the vehicle model over profile No. 1 at 30 m/s

FIGURE 11

Figure 12 shows the upper percentile levels of fatigue life use for tests on the two random road profiles and the largest peak value for the step response tests. In this graph, the computed fatigue life usage has been normalised by the fatigue damage (life usage) incurred at a point during the passage of a slowly moving (non-dynamic) vehicle.

Depending on the percentage of the road surface area considered in the analysis (the percentile level), the ratio of "dynamic" to "non-dynamic" fatigue damage may be in the range of 2-7 for normal highway conditions of speed and roughness. In other words, if (3) was a realistic damage criterion, a road designed with (3) using the static axle loads may be expected to fail in 1/2 - 1/7 of its design life, depending on the surface roughness and traffic conditions[1].

5.3 TENSILE STRAIN FATIGUE CRITERION

The maximum tensile strain in the roadway beam model was calculated at stations spaced at 150 mm intervals along the road, using the methods described in section 3. Strain time histories at each station along the road were determined (Fig-

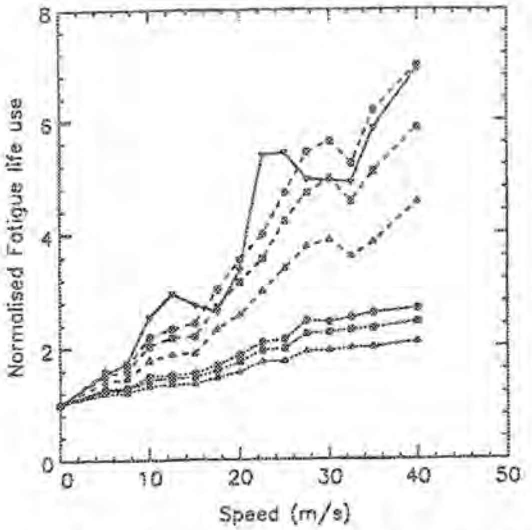

Normalised fatigue life usage (determined by the fatigue weighted stress criterion) due to passage of the vehicle model over the three road profiles (see legend Fig. 9)

FIGURE 12

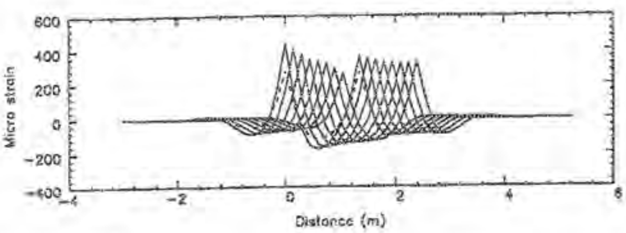

------ =Dynamic

- - - - = Non-dynamic (shown at one instant only)

Extreme fibre strains in the roadway model at closely spaced time intervals (animation) as it is traversed by the vehicle model at 30 m/s (tension = positive). Variation in the peak strain levels is caused by fluctuation of the wheel forces

FIGURE 13

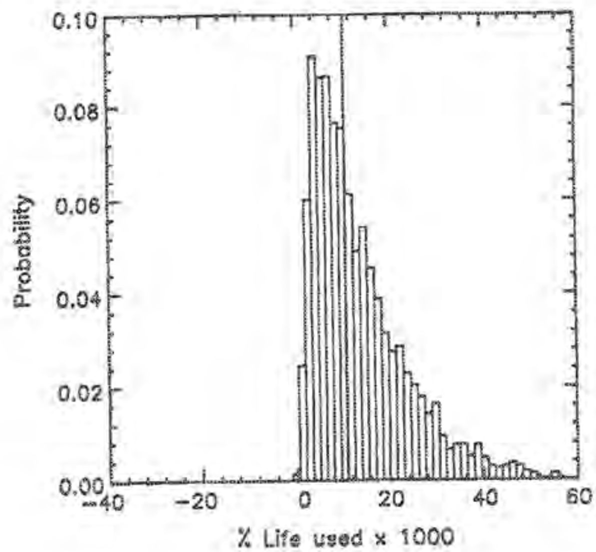

- · - · - - = Non-dynamic life usage

Probability distribution of tensile strain fatigue life usage along the road due to passage of the vehicle model (road profile No. 1, 30 m/s)

FIGURE 14

---

1 This does not account for the expected increase in dynamic wheel loads as the road surface profile degrades with incurred damage.

ure 13), and (5) was used to calculate the damage accumulation at each station. The probability distribution of this quantity is shown in Figure 14. Note the skewing of the distribution similar to that for the fatigue weighted stress criterion (Figure 9). The upper percentile levels (random profile tests) and largest peak values (step input tests) of the fatigue life usage have been normalised by the

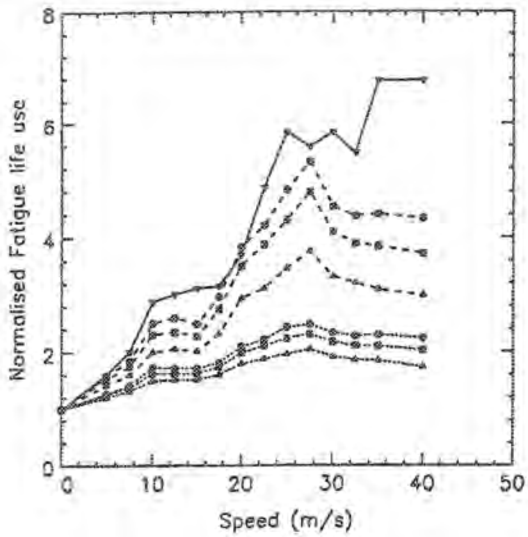

Normalised tensile strain fatigue life usage of the road surface due to passage of the vehilce model over the three road profiles (see legend Fig. 9)

FIGURE 15

"non-dynamic" fatigue damage and plotted in Figure 15. This figure is similar to Figure 12 except that the accumulated damage levels decrease for speeds above 25 m/s (random profile tests).

This is the result of two conflicting factors:

(i) The dynamic force levels increase with speed in this frequency range (see Figure 9).

(ii) The deflections of the road beam (and hence longitudinal strains) decrease with the speed of the load (see Figure 16). This phenomenon is known as the "speed effect" (23,49,55) and is discussed in more detail in (1).

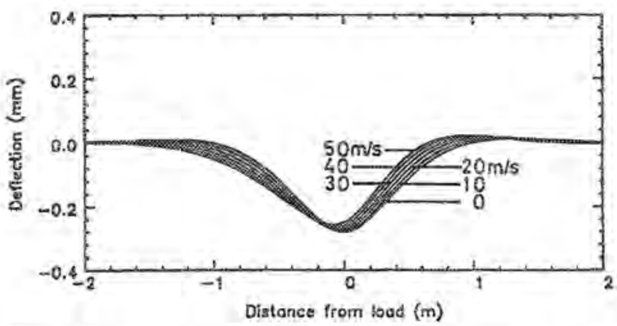

The effect of speed on beam deflections for a steady 40 kN load, located at x = 0, moving from left to right

FIGURE 16

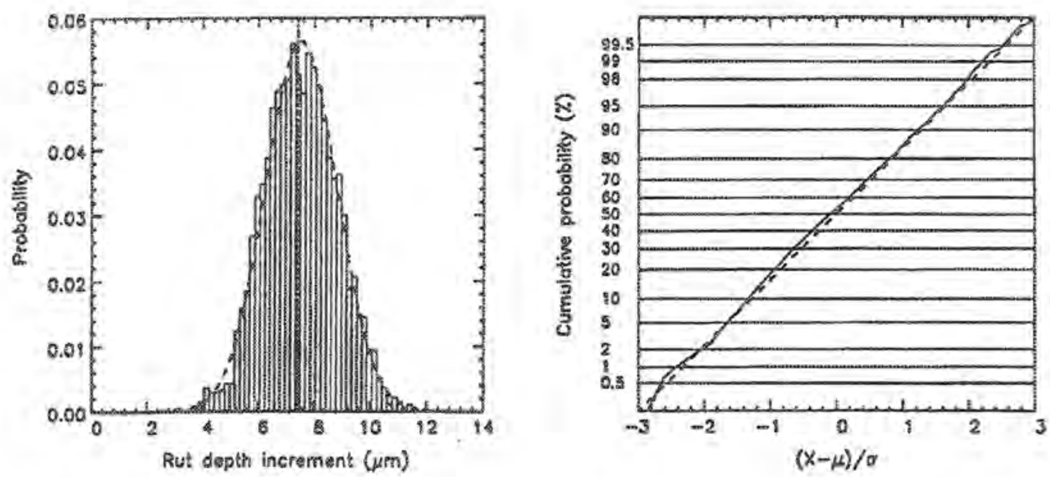

(a) Probability distribution (- - - - = Gaussain, — - — · — · — = Non-dynamic rut depth).

(b) Probability paper plot (- - - - = Gaussian).

Incremental permanent deformantion of the road surface due to passage of the vehicle model on profile No. 1 at 30 m/s

FIGURE 17

In this example, factor (ii) outweighs (i) and the net road damage accumulation decreases slightly with vehicle speed above 25 m/s. This is not the case for the step input tests where the dynamic force increase outweighs the effect of the road model response.

Typical values of the ratio of dynamic to "non-dynamic" fatigue life use vary between 2 and 7 for typical conditions of highway roughness and speed.

5.4 PERMANENT DEFORMATION CRITERION

The direct stress in the subgrade was calculated using the procedure described in section 3. The incremental permanent deformation was calculated at stations along the road using (8). The probability distribution is shown in Figure 17(a) and probability paper plot is shown in Figure 17(b) (30 m/s, Profile No. 1). The distribution is approximately Gaussian since the exponent in (7) is close to unity. The upper percentile levels (random tests) and largest peak values (step response tests) are shown in Figure 18. The values have been normalised by the "non-dynamic" permanent deformation. The results are similar to those obtained from the aggregate force calculation (Figure 9) except for the increasing gradient at speeds greater than 25 m/s. This can be attributed to the speed and frequency dependence of the subgrade stress. The ordinates of Figure 18 are similar to those of Figure 9 since in (7). As a result, the permanent deformation at a point is closely related to the aggregate force.

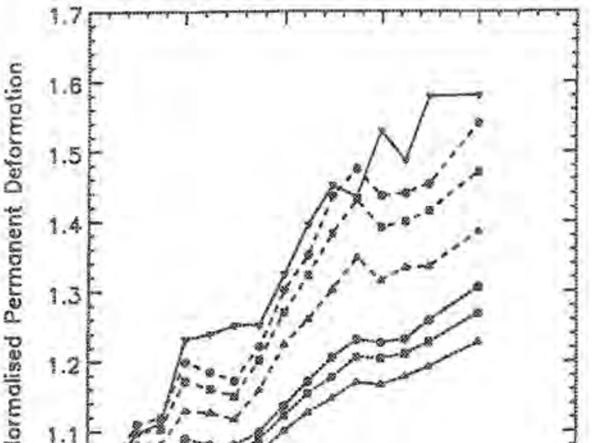

Normalised permanent deformation increments due to the passage of the vehicle model over the three road profiles (see legend Fig. 9)

FIGURE 18

Typical values of the dynamic permanent deformation are up to 60% greater than the "non-dynamic" values for typical conditions of highway roughness and speed.

6. CONCLUSIONS

(i) No suitable criteria were found in the literature for assessing dynamic wheel forces in terms of road surface damage.

(ii) Four road-damage-related wheel load criteria were developed. They consider the damage incurred at particular points along the road and must be evaluated from time histories of the forces generated by all axles of a vehicle. Two of the criteria require a mathematical model of transient roadway response. A method for calculating the time domain response of a linear roadway model (for which harmonic responses are known) to any number of moving random loads was described.

(iii) For vehicles operating on stationary random road surfaces typical of highways, road damage generally increases steadily with speed. Furthermore, there exist certain speeds at which pitch coupling between axles results in a significant increase in the damage incurred at particular points along the road. For the vehicle examined in this study, this coupling is provided by lightly damped pitching of the load levelling arrangement and the "critical" speeds were found to be approximately 9 m/s and 27 m/s. On smooth roads at high speeds the increase in dynamic wheel loads with speed is outweighed by the decrease in road surface response. The net effect is a reduction in road damage for speeds greater than 30 m/s.

(iv) The dynamic component of wheel forces may reduce significantly the service lives of road surfaces which are prone to fatigue failure. In particular the damage done to approximately five percent of the road surface during the passage of a vehicle at typical highway speeds may be increased by as much as a factor of four. When excessive permanent deformation is the most common mode of road surface failure, the service lives of roads may be reduced by at least 40% due to the dynamic component of the axle loads.

7. REFERENCES

1. Cebon, D. 'An Investigation of the Dynamic Interaction Between Wheeled Vehicles and Road Surfaces', PhD dissertation, University of Cambridge, 1985.

2. Fabian, G.J. 'An Outline and Preliminary Analysis of the Basic Problems of Road Loading Mechanics', Cornell Aeronautical Laboratory, Vehicle Dynamics Department, Report No. YM-1304-V-1, 1959.

3. Page, J. 'Dynamic Behaviour of a Single Axle Vehicle Suspension System: A Theoretical Study', TRRL Report LR580, 11p, Crowthorne, 1973 (Transport and Road Research Laboratory).

4. Page, J. 'Dynamic Behaviour of Two Linked-Twin-Axle Lorry Suspension Systems: A Theoretical Study', TRRL Report LR581, 21p, Crowthorne, 1973 (Transport and Road Research Laboratory).

5. Quinn, B.E., and Van Wyk, R. 'A Method for Introducing Dynamic Wheel Loads into Design of Roadways', Proc. Highway Research Board (40) 1961, pp 111-124.

6. Ervin, R.D. et al 'Influence of Size and Weight Variables on the Stability and Control Properties of Heavy Trucks', Chapter 4, 'Dynamic wheel load', University of Michigan Transportation Research Institute, Report No UMTRI-83-10-2, 1983.

7. Heath, A., and Good, M. 'Heavy Vehicle Design Parameters and Dynamic Pavement Loading', Australian Road Research 15(4) December, 1985 pp249-263.

8. Quinn, B.E., and Wilson, C.C. 'Can Dynamic Tire Forces Be Used as a Criterion of Pavement Condition', Highway Research Record No. 46, pp 88-100, 1964.

9. Sayers, M., and Gillespie, T.D. 'Dynamic Pavement/Wheel Loading for Trucks with Tandem Suspensions', Proc. 8th IAVSD Symposium on the Dynamics of Dehicles on Roads and on Railway Tracks, Cambridge, MA, 1983, pp 517-533, Swets & Zeitlinger, 1984.

10. Sweatman, P.F. 'A Study of Dynamic Wheel Forces in Axle Group Suspensions of Heavy Vehicles', Australian Road Research Board, Special Report SR No. 27, 56p, June 1983.

11. Whittemore, A.P., Wiley, J.R., Schultz, P.C., and Pollock, D.E. 'Dynamic Pavement Loads of Heavy Highway Vehicles', NCHRP Report 105, Highway Research Board, 1970.

12. Sayers, M., and Gillespie, T.D. 'The Effect of Suspension System Nonlinearities on Heavy Truck Vibration', 7th IAVSD Symposium on the Dynamics of Vehicles on Roads and on Tracks, Cambridge, 1981, pp 154-166, Swets & Zeitlinger.

13. Dickerson, R.S., and Mace, D.G.W. 'Dynamic Pavement Force Measurements with a Two-axle Heavy Goods Vehicle', TRRL Supplementary Report 688, 14p, Crowthorne (Transport and Road Research Laboratory).

14. Sweatman, P.F. 'Effect of Heavy Vehicle Suspensions on Dynamic Road Loading', Australian Road Research Board, Research Report ARR116, 15p, Dec. 1980.

15. Anon 'Impacts of Heavy Freight Vehicles', Organisation for Economic Cooperation and Development, December 1982.

16. Cady, J.B., and Aston, R.A.H. 'Vehicle Suspension Design to Reduce Road Damage', Automobile Engineer (London) V1, N1, 1975, pp 57-60.

17. Leonard, D.R., Grainger, J.W., and Eyre, R. 'Loads and Vibrations Caused by Eight Commercial Vehicles with Gross Weights Exceeding 32 tons (32.5 Mg)', TRRL Report LR582, 12p, Crowthorne, 1974 (Transport and Road Research Laboratory).

18. Page, J. 'A Review of Dynamic Loading Caused by Vehicle Suspensions', TRRL Supplementary Report 82UC, 16p, Crowthorne, 1974 (Transport and Road Research Laboratory).

19. Whiffin, A.C., and Leonard, D.R. 'A Survey of Traffic-induced Vibrations', RRL Report

LR418, 41p, Crowthorne, 1971 (Road Research Laboratory).

20. Bellini, W.R., and Thrower, E.N. 'A Digital Computer Program to Simulate the Passage of a Vehicle Over a Road Surface', RRL Report 181, 9p, Crowthorne, 1968, (Road Research Laboratory).

21. Potter, J.F. 'Dynamic Impact Pressures Generated under Roads by Sprung and Unsprung Vehicles', RRL Report LR137, 13p, Crowthorne, 1968 (Road Research Laboratory).

22. Savage, R.J. 'Dynamic Failure of Joints in Reinforced Concrete Pavements', Concrete, January 1985, 3p.

23. Anon 'The AASHO Road Test', Special Report No 61-E Pavement Research, Highway Research Board, Washington, 1962.

24. Rauhut, J.B., Roberts, F.L., and Kennedy, T.W. 'Response and Distress Models for Pavement Studies', Transp. Res. Rec. 715 TRB, 1979, pp 7-14.

25. Kennedy, T.W., Roberts, F.L., and Rauhut, J.B. 'Distress and Related Material Properties for Premium Pavements', Transp. Res. Rec. 715, TRB, 1979, pp 15-21.

26. Peattie, K.R. 'Flexible Pavement Design', Ch 1, Developments in Highway Pavement Engineering - 1. Applied Science Publishers Ltd., London, 1978, ed. Pell, P.S.

27. Brown, S.F. 'Material Characteristics for Analytical Pavement Design', Ch 2, Developments in Highway Pavement Engineering - 1. Applied Science Publishers Ltd., London, 1978, ed. Pell, P.S.

28. Thrower, E.N. 'A Parametric Study of a Fatigue Prediction Model for Bituminous Road Pavements', TRRL Report LR892, 19p, Crowthorne, 1979 (Transport and Road Research Laboratory).

29. Francken, L. 'Fatigue Performance of a Bituminous Road Mix under Realistic Test Conditions', Transp. Res. Rec. 712, TRB, 1979, pp 30-37.

30. Christison, J.T., Anderson, K.O., and Shields, B.P. 'In Situ Measurements of Strains and Deflections in a Full-depth Asphaltic Concrete Pavement', Proc. Assoc. Asphalt Paving Technology, V47, 1978, pp 398-430.

31. Lister, N.W., and Addis, R.R. 'Field Observations of Rutting and their Practical Implications', Transp. Res. Rec. 640 TRB, 1977, pp 27-34.

32. Zube, E., and Forsyth, R. 'An Investigation of the Destructive Effect of Floatation Tires on Flexible Pavement', Highway Res. Rec, HRB, N71, 1965, pp 129-150.

33. Maupin, G.W. 'Test for Predicting Fatigue Life of Bituminous Concrete', Transp. Res. Rec. 659, TRB, 1977, pp 32-37.

34. Raad, L., Monismith, C.L., and Mitchell, J.K. 'Fatigue Behaviour of Cement-treated Materials', Transp. Res. Rec. 641 TRB 1977, pp 7-11.

35. Goddard, R.T.N., Powell, W.D., and Applegate, M.W. 'Fatigue Resistance of Dense Bitumen Macadam: The Effect of Mixture Variables and Temperature', TRRL Suppl. Rep. 410, 26p, Crowthorne, 1978 (Transport and Road Research Laboratory).

36. Valkering, C.P. 'Effects of Multiple Wheel Systems and Horizontal Surface Loads on Pavement Structures', Proc. 3rd Int. Conf. Struct. Design Asph. Pav. Ann Arbor, 1972, pp 542-549.

37. Majidzadeh, K., Khedr, S., and El-Mojarrush, M. 'Evaluation of Permanent Deformation in Asphalt Concrete Pavements', Transp. Res. Rec. 715, TRB, 1979, pp 21-31.

38. Van de Loo, P.J. 'The Creep Test: A Key Tool in Asphalt Mix Design and in the Prediction of Pavement Rutting', Proc. Assoc. Asphalt Paving Technology, V47, 1978, pp 522-554.

39. Hunt, H.E.M. 'A Preliminary Investigation into the Response of Semi-infinite Continua to Moving Dynamic Surface Forces'. Cambridge University Engineering Dept. Project Report, 1985.

40. Achenback, J.D., Keshava, S.P., and Hermann, G. 'Moving Load on a Plate Resting on an Elastic Half Space'. Trans. ASME J. Ap-

plied Mechanics, December 1967, pp 910-914.

41. Fryba, L. 'Vibration of Solids and Structures under Moving Loads', Noordhoff International Publishing, Groningen, Netherlands, 1972.

42. Grassie, S.L., Gregory, R.W., Harrison, D., and Johnson, K.L. 'The Dynamic Response of Railway Track to High Frequency Vertical Excitation', J. Mech. Eng. Sci. V24, No 2, 1982, pp 77-90.

43. Huang, T.C., and Shah, V.N. 'Elastic System Moving on an Elastically Supported Beam', J. Vibration, Accoustics, Stress and Reliability in Design, (ASME Trans) V106, April 1984, pp 292-297.

44. Le Houedec, D. 'Response of a Roadway Lying on an Elastic Foundation to Random Traffic Loads', J. Applied Mechanics, (ASME Trans) V47, pp 145--149, March 1980.

45. Shah, V.N., Cook, R.D., and Huang, T.C. 'Loads Moving on Beam Supported by Layered Elastic Foundation', J. Mechanical Design, (ASME Trans) V102, pp 295-302, April 1980.

46. Holder, B.W., and Michalopoulos, C.D. 'Response of a Beam on an Inertial Foundation to a Travelling Load', AIAA Journal, V15, no 8, August 1977, pp 1111-1115.

47. Battiato, G., Verga, C., and Ronca, G. 'Viscoelastic Deformations in a Two Layered Paving System Predicted from Laboratory Creep Results', Transp. Res. Rec. 640 TRB, 1977, pp34-38.

48. Ferrari, P. 'Calculation of the Deformations Caused by Vehicles to Flexible Pavements'. Proc. 3rd. Int. Conf. Structural Design of Asphalt Pavements. University of Michigan, Ann Arbor, 1972, pp 382-391.

49. Ishihara, K., and Kimura, T. 'The Theory of Viscoelastic Two-layer Systems and Conception of Its Application to the Pavement Design'. Proc. 2nd. Int. Conf. Structural Design of Asphalt Pavements. University of Michigan, Ann Arbor, 1967. pp 245-254.

50. Westmann, R.A. 'Viscoelastic Layered System Subjected to Moving Loads', Proc. ASCE, J. Engineering Mechanics Div. EM3, pp 201-218, June 1967.

51. Harris, F.J. 'On the Use of Windows for Harmonic Analysis with the Discrete Fourier Transform', Proc. IEEE, V66, N1, Jan. 1978, pp 51-58.

52. Cebon, D., 'Heavy Vehicle Vibration - A Case Study', Proc. 9th IAVSD Symposium on the Dynamics of Vehicles on Roads and on Tracks, Linkoping, Sweden, 1985, Swets and Zeitlinger.

53. Anon. 'Proposals for Generalised Road Inputs to Vehicles', ISO/TC 108/WG9 draft No. 3e, May 1972.

54. Cebon, D., and Newland, D.E. 'The Artificial Generation of Road Surface Topography by the Inverse FFT Method', Proc. 8th IAVSD Symposium on the Dynamics of Vehicles on Roads and on Railway Tracks, Cambridge, MA, 1983, pp 29-42, Swets & Zeitlinger, 1984.

55. Harr, M.E. 'Influence of Vehicle Speed on Pavement Deflections', Proc. Highway Research Board, No 41, 1962, pp 77-82.